Dalton Transactions

Identification of Key Functionalization Species in the Cp*Ir(III)-Catalyzed-Ortho Halogenation of Benzamides

Journal:	*Dalton Transactions*
Manuscript ID	DT-ART-02-2020-000565.R2
Article Type:	Paper
Date Submitted by the Author:	10-Apr-2020
Complete List of Authors:	Ison, Elon; North Carolina State University, Chemistry Guzmán Santiago, Alexis; North Carolina State University, Chemistry Brown, Caleb; North Carolina State University, Chemistry Sommer, Roger; North Carolina State University, Chemistry

ARTICLE

Identification of Key Functionalization Species in the Cp*Ir(III)-Catalyzed-*Ortho* Halogenation of Benzamides.

Received 00th January 20xx,
Accepted 00th January 20xx

DOI: 10.1039/x0xx00000x

Alexis J. Guzmán Santiago[a], Caleb A. Brown[a], Roger D. Sommer[a], and Elon A. Ison[a]*

Abstract: Cp*Ir(III) complexes have been shown to be effective for the halogenation of *N*,*N*-diisopropylbenzamides with N-halosuccinimide as a suitable halogen source. The optimized conditions for the iodination reaction consists of 0.5 mol% $[Cp^*IrCl_2]_2$ in 1,2-dichloroethane at 60 °C for 1 h to form a variety of iodinated benzamides in high yields. Increasing the catalyst loading to 6 mol% and the time to 4 h enabled the bromination reaction of the same substrates. Reactivity was not observed for the chlorination of these substrates. A variety of functional groups on the *para*-position of the benzamide were well tolerated. Kinetic studies showed the reaction dependence is first order in iridium, first order in benzamide, and zero order in *N*-iodosuccinimide. A KIE of 2.5 was obtained from an independent H/D kinetic isotope effect study. Computational studies (DFT-BP3PW91) indicate that a CMD mechanism is more likely than an oxidative addition pathway for C–H bond activation step. The calculated functionalization step involves an Ir(V) species that is the result of oxidative addition of acetate hypoiodite that is generated *in situ* from *N*-iodosuccinimide and acetic acid.

Introduction

Directed catalytic C–H bond activation has become a valuable strategy for the synthesis of functionalized molecules and has been exploited for the development of numerous C–C bond forming reactions.[1] There have been significant advances in the development of both selective and catalytic C–heteroatom (O, N), and C–X (X = halogen) bond forming reactions.[2,3] Organic halides are commonly used as electrophiles in substitution reactions, as core building blocks for the synthesis of nucleophilic organometallic reagents, like Grignard reagents,[4] and as suitable substrates for numerous cross-coupling reactions.[5] In addition, the C(sp^2)–X motif plays a key role in the properties of many natural products,[6] agrochemicals[7] and pharmaceuticals.[5] Therefore, the need for general direct C–H bond halogenation strategies is evident.

[Cp*Rh(III)] complexes have been well established as a suitable catalyst for the activation and functionalization of otherwise inert C–H bonds. For example, the Glorius group reported a high-yielding and versatile [Cp*Rh(III)]-catalysed system for the *ortho*-halogenation of a variety of benzene and acrylic acid derivatives, as well as (electron-rich) heterocycles. [3a, 3c] Despite these advances, several questions remain about the mechanism for this reaction. For example, the mechanism is believed to proceed via a cyclometalated intermediate that arises from C-H activation of the substrate. However, this type of intermediate has not been isolated and examined for its catalytic activity. Further, it is not clear whether C-H activation occurs prior to, or after the activation of the halogen source. In addition, there have been conflicting reports with regards to the existence of a Rh(V) intermediate which can undergo reductive elimination to generate the desired product or whether, dependent on the substrate, as suggested by Lan and co-workers, the reaction proceeds through a Rh(III) species and a bromonium intermediate.[8]

More recently, the Martin-Matute group developed a [Cp*Ir(III)] system for the mild iodination of benzoic acids.[3j] The solvent hexafluoroisopropanol (HFIP) was proposed to aid in lowering the energy barrier for the rate determining step (RDS) of the reaction (Scheme 1). Also, our group has demonstrated catalytic C–H bond activation by H/D exchange experiments could be achieved with a variety of [Cp*Ir(III)] complexes.[9] This work led to the catalytic C–H bond activation and functionalization of benzoic acids with benzoquinones and alkynes to form the respective benzochromenones[10] and isocoumarins. [1o] Herein, we report the conditions for the Cp*Ir-catalysed halogenation of benzamides with *N*-halossuccinimides as the halogen source (Scheme 1).

[a] *Department of Chemistry, North Carolina State University, 2620 Yarborough Drive, Raleigh North Carolina 27695-8204, United State.*

Electronic Supplementary Information (ESI) available: Additional kinetic and computational data as well as Crystallographic data. CCDC 1982446−1982448 for ESI and crystallographic data in CIF or other electronic format see DOI: 10.1039/x0xx00000x.

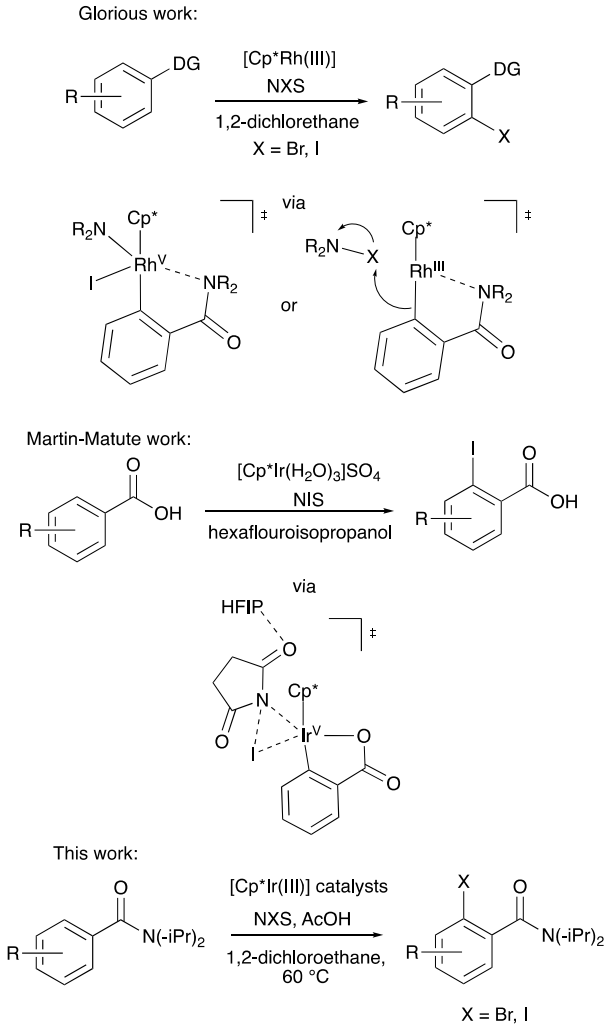

Scheme 1. Summary of previous and current work.

Results and Discussion

Substrate Scope. The optimal reaction conditions for the synthesis of halogenated product **2a** were utilized for a variety of *para*-substituted benzamides (Scheme 2). Overall both electron donating and electron withdrawing groups were well tolerated under the optimized reaction conditions. In general, electron rich substrates resulted in better yields than electron poor substrates. It is worth noting that the 4-methoxy-*N*,*N*-diisopropylbenzamide was low yielding. Although we are still trying to rationalize this, the same result was observed in previous work focused on the Cp*Ir(III)-catalysed synthesis of isocoumarins.[10]

Based on the success of the iodination reaction, the analogous bromination reaction using *N*-bromosuccinimide (NBS) as the halogen source was pursued. The reaction proceeded smoothly with NBS as a suitable halogen source. Higher catalyst loadings (6 mol%), and reaction times (4 h) were required for full conversion of the model substrate **1a**. A variety of *para*-substituted benzamides was tolerated under the optimized reaction conditions and the yields for a series of brominated products are shown in Scheme 3. It is worth mentioning that lower yields were observed overall for all substrates for the bromination reaction. This is particularly true for the napthyl substituted substrate, as no product was detected by ^{1}H-NMR spectroscopy or GC.

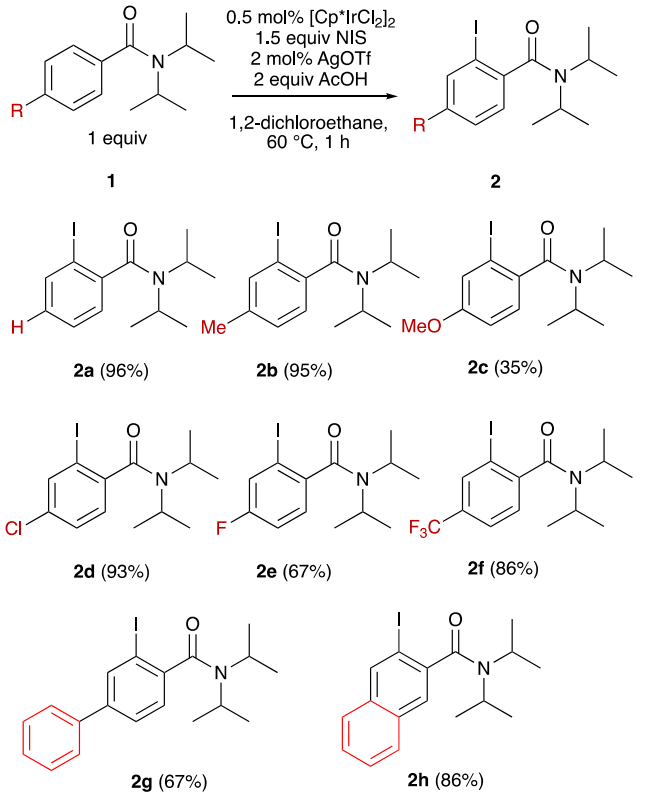

Scheme 2. Substrate scope for the iodination of benzamides.

Mechanistic Studies. Kinetic data for the catalytic reaction was obtained by gas chromatography (GC). For these studies **1a** was used as the model substrate. The reaction was observed to have a positive order dependence with respect to **1a**, and iridium, and approximately a zeroth order dependence on N-iodosuccinimide (See Supporting Information). Traditionally, proposed mechanisms for directed C–H activation begin with coordination of the substrate to the metal centre, followed by C–H activation.

An H/D kinetic isotope effect experiment was undertaken to determine if C–H activation occurs prior to or during the turnover limiting step of the reaction. The rate of the reaction was measured independently using **1a** and d_5-*N*,*N*-diisopropylbenzamide. The reaction with d_5-benzamide was found to be approximately half as fast as the reaction with the fully proteated substrate, resulting in a KIE (k_H/k_D) of 2.5. The observed value for the KIE is significant and suggests that C–H activation occurs prior to or in the turnover limiting step for the mechanism.[11]

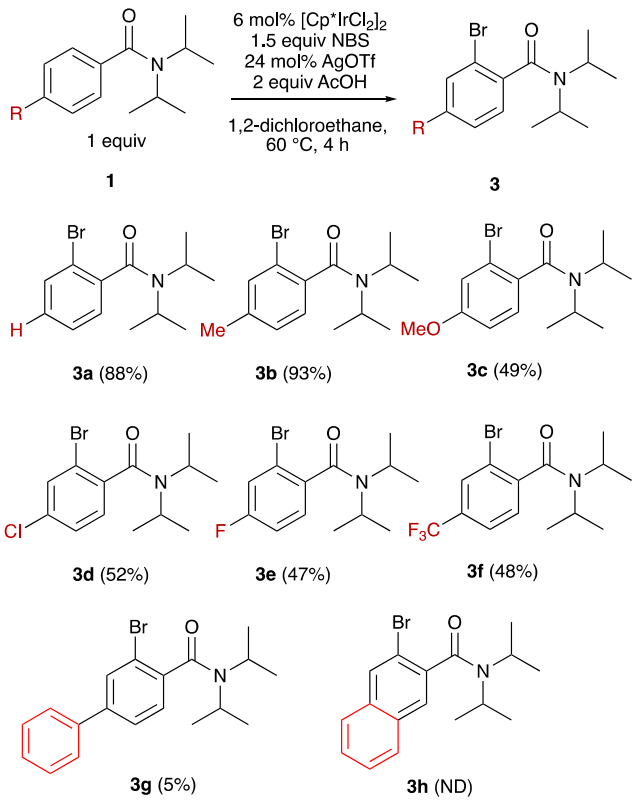

Scheme 3. Substrate scope for the bromination of benzamides.

Mechanistic Proposal. Based on the data, two preliminary mechanisms are proposed where the functionalization step differs in the halogen source. The first mechanism begins with chloride abstraction of the $[Cp^*IrCl_2]_2$ by AgOTf to generate the active $Cp^*Ir(OAc)_2$ complex **4**. Benzamide coordination then occurs displacing the κ_1 acetate ligand to form complex **5**. C–H activation can then occur to form the cyclometalated iridacycle **6** with the formation and loss of acetic acid. Incoming halosuccinimide then coordinates to the iridium centre to form complex **7.** Halogenation then occurs to form complex **8**. Two equivalents of acetic acid regenerate the active Cp*Ir(III) complex (Scheme 4).

The lack of an observed dependence in iodosuccinimide suggests that this species may not be the active halogen source. An alternative mechanism is proposed, where a acetyl hypohalite is produced *in situ,* from an off-cycle equilibrium between acetic acid and the halosuccinimide, and this species acts as the active halogen source. This acetyl hypohalite can coordinate to the iridium centre to form complex **9.** Upon coordination, halogenation of the substrate occurs to form **10**. One equivalent of acetate completes the catalytic cycle and regenerates the Cp*Ir(III) catalyst (Scheme 5).

Isolation of Complex 6(DMSO). An analogous cyclometalated complex to the proposed complex **6**, stabilized by DMSO has been successfully synthesized and characterized (Scheme 6). A 1:1:1 ratio of $Cp^*Ir(DMSO)Cl_2$, *N,N*-diisopropylbenzamide and acetic acid was treated with two equivalents of silver triflate, to abstract the chlorides from the iridium complex and generate the cyclometalated complex, **6(DMSO)** as a yellow solid in 90%

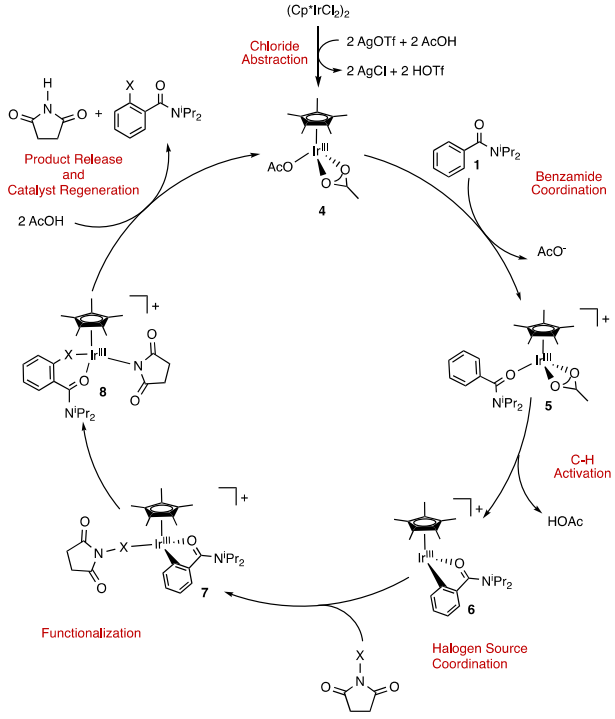

Scheme 4. Proposed mechanism for the halogenation of benzamides Involving NXS as the active halogen source.

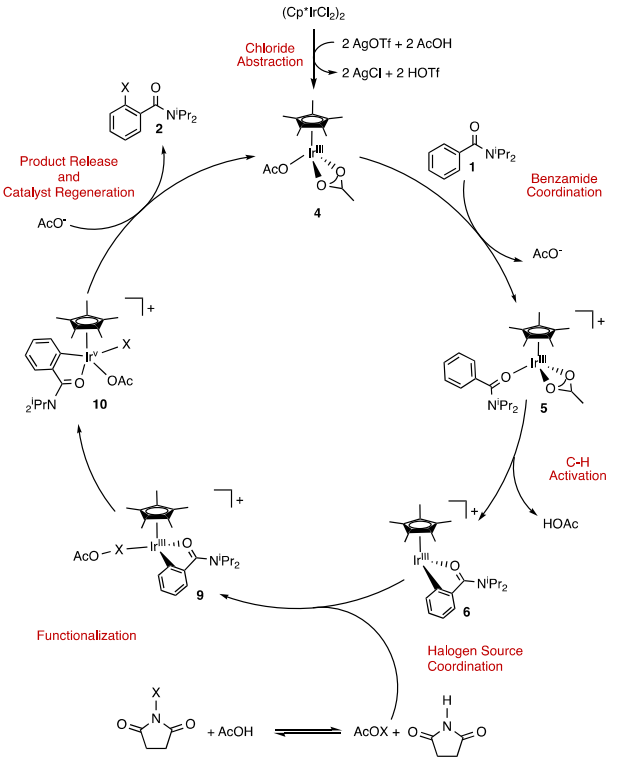

Scheme 5. Proposed mechanism for the halogenation of benzamides Involving X(OAc) as the active halogen source.

yield (Scheme 6). This complex has been characterized by ^1H, ^{13}C-NMR spectroscopy, elemental analysis (See Supporting Information). The X-ray crystal structure for **6(DMSO)** is shown in Figure 1. Bond lengths and angles are similar to the analogous

complex with a benzoate ligand that has been previously

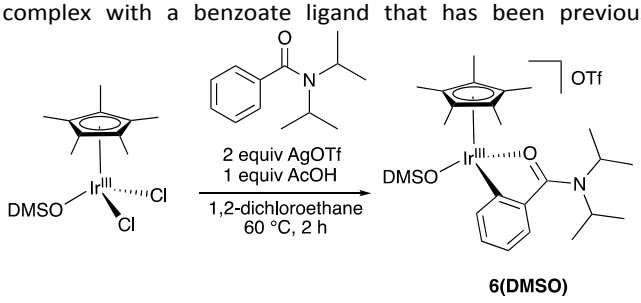

Scheme 6. Synthesis of complex **6(DMSO)**

reported by our group.[1o]

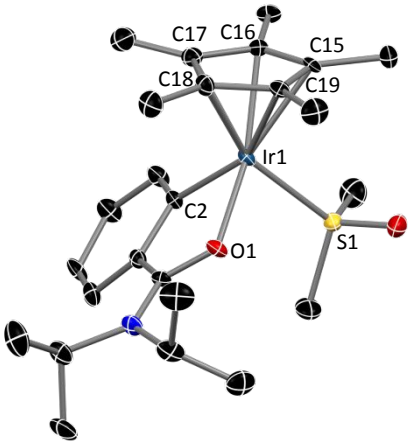

Figure 1. Thermal ellipsoid plot (50% ellipsoids) of the cationic fragment of **6(DMSO)**. The triflate anion is omitted for clarity. Selected bond lengths (Å): Ir1-S1, 2.267; Ir1-O1, 2.115; Ir1-C2, 2.036; Ir1-Cp*(average), 2.209.

Stoichiometric Halogenation. Recently, hypervalent iodine reagents (Chart 1) have gained interests in the synthetic community for the oxidative functionalization of hydrocarbons as an alternative source of electrophilic iodine.[12] In this class of reagent, dioxoiodanes have been shown to be effective in the oxyiodination of alkenes and alkynes, where the proposed active halogen source is an acetyl hypoiodite monomer generated *in situ* from the acid promoted decomplexation of such reagents.[13]

Acetyl hypoiodite has also been proposed in earlier work by Colobert and coworkers,[12a] and it was shown that a variety of electron-rich substrates can be readily iodinated by NIS in the presence of catalytic amounts of trifluoroacetic acid. Based on this work, the reactivity of **6(DMSO)** towards both acetyl hypoiodite and NIS as potential halogen sources in the reaction was investigated.

Acetyl hypoiodite, **11**, was generated *in situ* from molecular iodine and silver acetate. The presence of **11** was confirmed by ^{1}H-NMR spectroscopy (Supporting Information). This mixture, with a known concentration of **11**, was then filtered and added to a solution of **6(DMSO)**. A ^{1}H-NMR spectrum of the crude reaction mixture shows clear product formation after the reaction time (Figure 2).

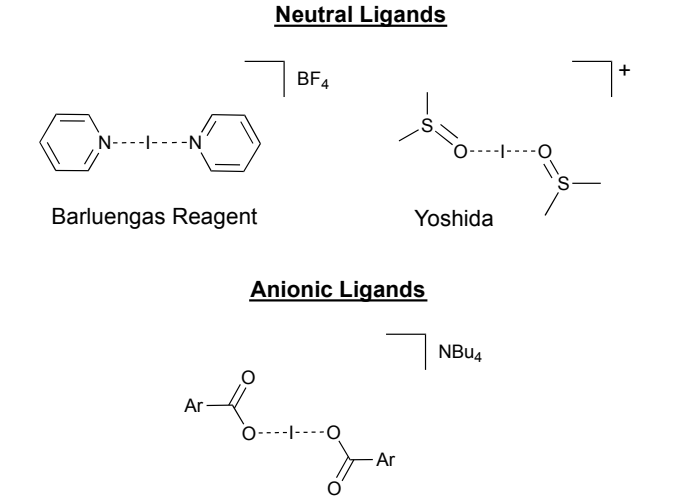

Chart 1. Examples of stable iodine(I) compounds.

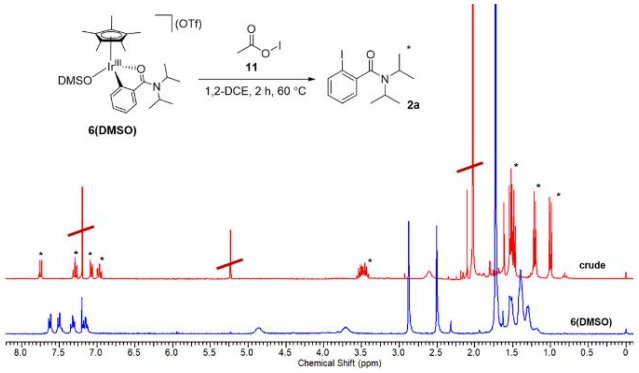

Figure 2. ^{1}H-NMR spectrum for the reaction of **11** (generated in situ) with **6(DMSO)**. The blue spectrum is the spectrum for **6(DMSO)** before the addition of the halogenation source. The red spectrum is the spectrum after the addition of **11** (generated in situ) and heating the solution for 2 h. Signals for the organic product are indicated with an asterisk.

From the ^{1}H-NMR spectrum of a solution containing *N*-halosuccinimide with tetrabutylammonium acetate (TBAOAc), a

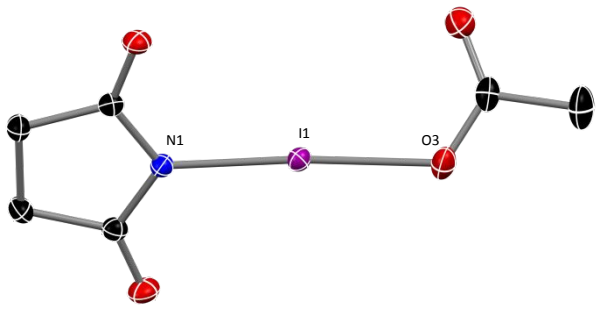

Figure 3. Thermal ellipsoid plot (50% ellipsoids) for the anion in $[(C_4H_4O_2N)I(OCOCH_3)][Bu_4N]$, **12**. The cation has been omitted for clarity. Selected bond lengths (Å) and angles: N1-I1-O3, 174°; I1-O3, 2.293; I1-N1, 2.166. Tetrabutylammonium counterion is not shown for clarity.

shift can be observed for the signal corresponding to the methyl of the acetate group from 1.95 ppm (TBAOAc) to 2.70 ppm (NIS) and to 2.85 ppm for NCS (See Supporting Information). The

corresponding complex from NIS and TBAOAc, **12**, was further characterized by ^{13}C-NMR and X-ray crystallography (See Supporting Information) and the crystal structure of **12** is shown in **Figure 3**. As expected, the structure features an approximately linear geometry (174°) around the central iodine atom. The iodine-oxygen bond length is significantly longer (2.29 Å) than the analogous benzoate complexes reported by Muniz and co-workers (2.16 - 2.20 Å).

Complex **12** was examined as a halogen source (Table 1). In the absence of a proton source very little reactivity was observed, Table 1 (entry 1). When a polar protic solvent was utilized, or two equivalents of H_2O, were included as an additive, significant yields of **2a** from complex **6(DMSO)** were observed (entries 3 - 10). These results suggest that an acidic proton is needed to generate the active I(OAc) species in situ. It should also be noted that protic sources with coordinating counterions like acetate could result in the formation of other stabilized complexes which are less reactive. This was demonstrated when $[I(OAc)_2]$(TBA) (Table 1, entry 2) was utilized. Moreover, a bis-succinimide stabilized complex was identified by X-ray crystallography in the reaction of NIS with TBAOAc (See Supporting Information).

Table 1. Stoichiometric reactivity for **12** with **6(DMSO)**

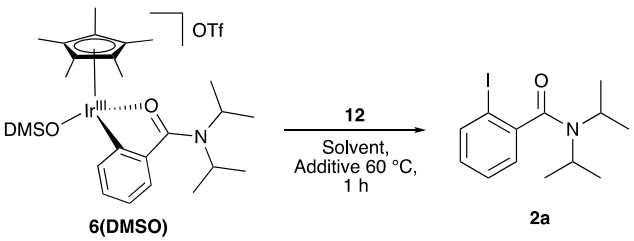

6(DMSO) **2a**

Entry[a]	Solvent	Additive	% conversion
1	1,2-dichloroethane	-	10[b]
2	1,2-dichloroethane	-	Traces[c]
3	1,2-dichloroethane[d]	2 equiv H_2O	63
4	MeCN	-	20
5	MeCN	2 equiv H_2O	37
6	MeOH	-	27
7	MeOH	2 equiv H_2O	34
8	^{t}AmylOH	-	52
9	^{t}AmylOH	2 equiv H_2O	75
10	^{t}AmylOH	2 equiv TFAA[d]	29

[a]General reaction conditions: 15 mg (0.02 mmol) of **6(DMSO)**, (0.02 mmol) of the halogen source, and (0.04 mmol) of an additive in 1 mL of 1,2-dichloroethane under air. Percent conversion was determined by GC with the use of hexafluorobenzene as an internal standard. [b]Reaction was carried out under the optimized reaction conditions using **12**. [c]The halogen source was changed to $[I(OAc)_2]$(TBA). [d]TFAA = trifluoroacetic acid.

Computational Mechanistic Analysis.

The formation of the proposed acetyl hypohalite by the association of acetate anion with NXS (X = Cl, Br, I) was modelled computationally (Figure 4). The association to form **12** is exergonic ($\Delta G°$ = -5.9 kcal/mol) for X = I, but endergonic for X = Br ($\Delta G°$ = 10.8 kcal/mol) and X = Cl, ($\Delta G°$ = 14.5 kcal/mol). The results are consistent with the observed catalytic reactions as iodination was most facile, followed by bromination (which required higher temperature and catalysts loadings). However, chlorination was not observed under any catalytic conditions.

C–H Activation. For the C-H activation step of the mechanism, both a (concerted-metalation-deprotonation) CMD[14] and a direct oxidative addition pathway were considered (Figure 5). Starting from a proposed iridium bisacetate, **INT-1**, addition of benzamide was considered via one of two coordination modes to yield **INT-2** and **INT-3**. Benzamide coordination through the oxygen resulted in **INT-2** ($\Delta G°$ = 15.7 kcal/mol). Alternatively,

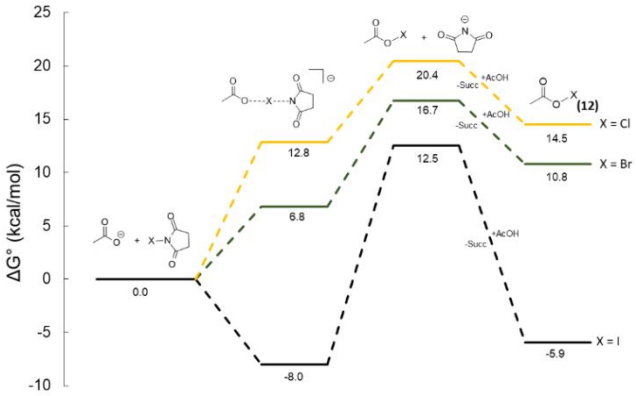

Figure 4. DFT (B3PW91-D3) calculated energetics for the association of acetate anion (OAc) with *N*-halosuccinimide in 1,2-dichloroethane solvent.

coordination of benzamide through the nitrogen yields **INT-3** ($\Delta G°$ = 42.8 kcal/mol). **INT-3** is too high in energy compared to **INT-2**, which suggests that oxygen coordination is more likely. The CMD pathway for C–H bond activation can occur through **TS-1** ($\Delta G^‡$ = 24.9 kcal/mol). On the other hand, the oxidative addition pathway resulted in a ground state energy for **INT-4** at 41.2 kcal/mol. The high energy of this intermediate (**INT-4**) indicates that this pathway is unlikely for C–H bond activation. Thus, the acetate assisted CMD pathway is lower in energy than that the oxidative addition pathway and is more likely to occur for C–H bond activation.

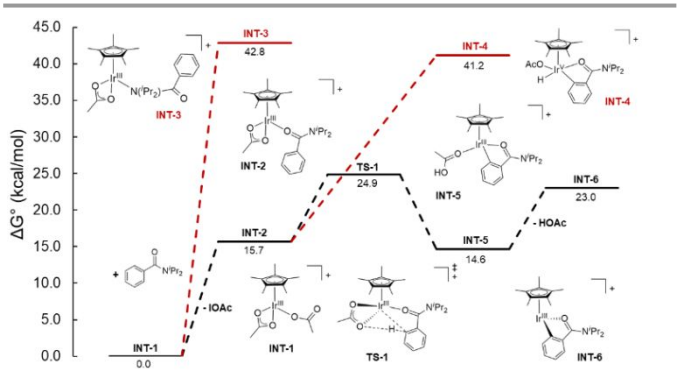

Figure 5. DFT (B3PW91-D3) calculated energetics for the C-H activation step in 1,2-dichloroethane.

Functionalization with *N*-iodosuccinimide. The functionalization with *N*-iodosuccinimide was explored in Figure 6. Addition of *N*-iodosuccinimide to **INT-6** results in **INT-7**. Oxidative addition of the coordinated NIS occurs through **TS-2** with an associated energy of 35.5 kcal/mol, to yield an Ir(V) iodide complex **INT-8** (ΔG° = 8.2 kcal/mol). This step is followed by reductive elimination through **TS-3** with an energy barrier of 29.1 kcal/mol, and results in **INT-9** (ΔG° = -8.9 kcal/mol). Product release from **INT-9** and protonation with acetic acid results in the regeneration of the catalyst through **TS-4** (21.4 kcal/mol).

Functionalization with iodoacetate. The viability of generating acetyl hypohalite under our reaction conditions has been demonstrated experimentally, therefore a pathway using acetyl hypoiodite as the halogen source was investigated (Figure 7). Even though iodine coordination is favoured over oxygen coordination (**INT-14** is lower in energy than **INT-15** by 13.7 kcal/mol), the barrier for oxidative addition is lower for the oxygen bound acetyl hypoiodite with a TS energy (**TS-7**) of 28.2 kcal/mol compared to **TS-5** ($\Delta G^{\ddagger}$ = 35.3 kcal/mol). Oxidative addition will yield **INT-16** (ΔG° = 5.0 kcal/mol). From there reductive elimination can occur through **TS-8** (14.8 kcal/mol) to yield **INT-17** (ΔG° = -7.4 kcal/mol). To complete the catalytic cycle product is released to regenerate **INT-13**. On the other hand, the direct functionalization pathway remains unfavourable for the acetyl hypoiodite pathway due to the high energy associated with **TS-6** ($\Delta G^{\ddagger}$ = 36.8 kcal/mol). An alternative functionalization mechanism that was pursued involved the formation of acetyl hypoiodite in situ, which acts as the substrate for iodination (vide supra). From **INT-6**, initial NIS coordination through the N-I bond was found to be the most favourable coordination mode.

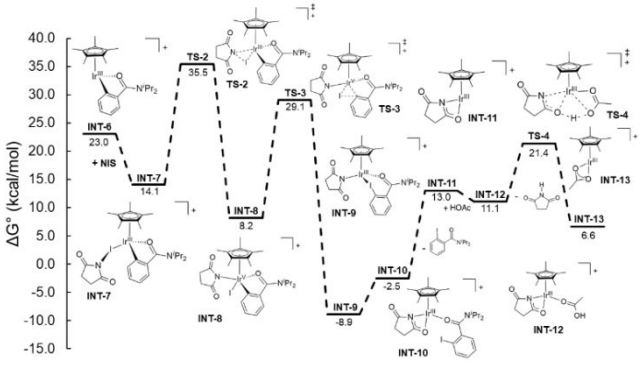

Figure 6. DFT (B3PW91-D3) calculated energetics for the Ir(III)-catalysed iodination with *N*-iodosuccinimide in 1,2-dichloroethane.

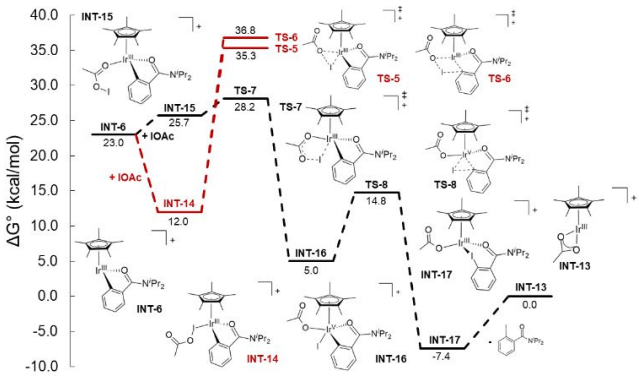

Figure 7. DFT (B3PW91-D3) calculated energetics for the Ir(III)-catalysed iodination with I(OAc) in 1,2-dichloroethane.

Computational data support a mechanism where the iodosuccinimide reacts with acetic acid to generate acetyl hypoiodite *in situ which serves as the halogen source.* C–H bond activation occurs through a CMD type mechanism and the halogenation of the substrate appears to proceed through an Ir(V) intermediate which is formed as the oxidative addition product of the cyclometalated iridacycle (**INT-6**) and the acetyl hypoiodite. To account for the differences in reactivity between NIS, NBS and NCS we compared the energies for the oxidative addition of the acetyl hypoiodite with each halogen (Figure 8). From Figure 8, there is a substantial difference between the oxidative addition of XOAc dependent on the halogen. The oxidative addition for IOAc proceeds through an accessible barrier of 26.9 kcal/mol, whereas the chlorination reaction was not observed experimentally and proceeds through a calculated barrier of 33.1 kcal/mol (**TS-7**). The increased catalyst loading, and the reaction times required for the bromination reaction are also consistent with a calculated energy for **TS-7** of 28.2 kcal/mol.

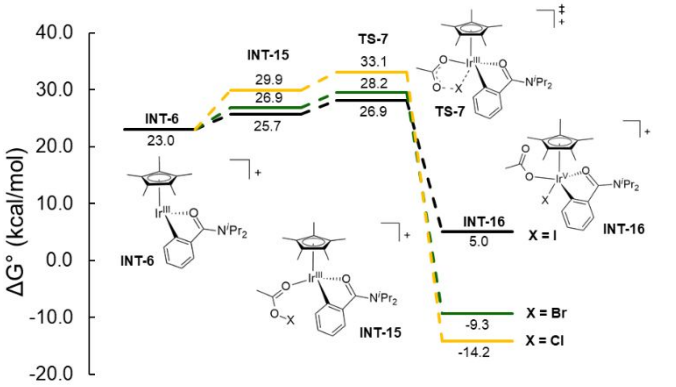

Figure 8. DFT (B3PW91-D3) calculated energetics for the oxidative addition of X(OAc) (X = halide) in 1,2-dichloroethane.

Conclusions

The Cp*Ir(III) catalysed halogenation of benzamides using *N*-iodosuccinimides has been optimized and probed mechanistically. A variety of *para*-substituted benzamides were well tolerated by this reaction. Additionally, the reaction was adapted to enable the analogous bromination reaction. It was determined that the catalytic reaction has a first order dependence in iridium, a positive dependence in benzamide and an approximately zero order dependence in *N*-iodosuccinimide. Based on these data two reaction mechanisms were proposed, which differ solely on the nature of the halogen source. These were then investigated computationally. It was demonstrated that the formation of acetyl hypoiodite is favourable under our reaction conditions. Furthermore, for the C–H bond activation step, an acetate-assisted CMD mechanism was found to be more likely than an oxidative addition mechanism due to the high ground state energy of the intermediates for the oxidative addition pathway. Computational results suggest that functionalization from acetyl hypoiodite formed *in situ* is favoured over direct *N*-

iodosuccinimide functionalization due to the difference in barriers for the oxidative addition of these (acetyl hypohalite and *N*-halosuccinimide) substrates. Finally, experimental evidence supporting the proposed acetyl hypoiodite pathway with a series of stoichiometric studies has been provided. Thus, the implications of this study are that directed functionalization of the benzamide substrates utilized here is facilitated by the ease of oxidative addition of the halogenating substrate. This result is important for the further development of methods for the halogenation of aromatic substrates.

Experimental

General Considerations.

$IrCl_3 \cdot 3H_2O$ was purchased from Pressure Chemical Company. The following Ir complexes: $[Cp^*IrCl_2]_2$,[15] $Cp^*Ir(Me_2SO)(OAc)_2$,[10] $Cp^*Ir(NHC)(Cl_2)_2$,[10] and $[Cp^*Ir(H_2O)_3]OTf_2$[16] were prepared as previously reported. All other reagents were purchased from commercial sources and used as received unless stated otherwise. All reactions were performed under air and using non-dry solvents unless otherwise noted. ^1H and ^{13}C NMR spectra were obtained at room temperature on a Varian Mercury 400 MHz spectrometer or a Varian Mercury 300 MHz spectrometer. Chemical shifts are listed in parts per million (ppm) and referenced to their residual protons or carbons of the deuterated solvents. Gas chromatography (GC) was performed on a Varian 3800 Gas Chromatograph with a Varian VF-53ms column. Elemental analyses were performed by Atlantic Micro Labs, Inc.

General Procedure for the Iridium Catalysed Iodination of Benzamides.

A foil covered screw cap test tube with a magnetic stirrer was charged with benzamide (1 mmol, 1.0 equiv), *N*-iodosuccinimide (1.5 mmol, 1.5 equiv), $[Cp^*IrCl_2]_2$ (0.005 mmol, 0.5 mol%), silver triflate (0.02mmol, 2 mol%), acetic acid (2 mmol, 2 equiv) and 1 mL of 1,2-dichloroethane. The reaction mixture was stirred at 60 °C for 1 hour in an oil bath. Upon completion, the solution was diluted with dichloromethane and filtered through celite. The solvent was removed under reduced pressure and the crude reaction mixture was purified by column chromatography on silica gel.

General Procedure for the Iridium Catalysed Bromination of Benzamides.

A foil covered screw cap test tube with a magnetic stirrer was charged with benzamide (1 mmol, 1.0 equiv), *N*-bromosuccinimide (1.5 mmol, 1.5 equiv), $[Cp^*IrCl_2]_2$ (0.06 mmol, 6 mol%), silver triflate (0.24mmol, 24 mol%), acetic acid (2 mmol, 2 equiv) and 1 mL of 1,2-dichloroethane. The reaction mixture was stirred at 60 °C for 4 hours in an oil bath. Upon completion, the solution was diluted with dichloromethane and filtered through celite. The solvent was removed under reduced pressure and the crude reaction mixture was purified by column chromatography on silica gel.

Synthesis of $Cp^*Ir(DMSO)(C_{13}H_{19}NO)$ (6(DMSO)).

In a 5 mL storage tube equipped with a stir bar, was added $Cp^*Ir(DMSO)Cl_2$ (119 mg, 0.25 mmol), N,N-diisopropylbenzamide (51.3 mg, 0.25 mmol), acetic acid (2 equiv, 28.6 µL), and AgOTf (2 equiv, 128.5 mg) to 1,2-dichloroethane (2 mL) and stirred at 60 °C for 1 h. The crude reaction mixture was then filtered and concentrated under reduced pressure to remove excess solvent. The resulting residue was dissolved in minimal dichloromethane. To the concentrated dichloromethane solution excess pentane was added to afford a yellow precipitate. The precipitate was filtered to afford a yellow powder in 90% yield. ^1H-NMR (300 MHz, $CDCl_3$) δ (ppm): 7.68 (d, J = 6.0 Hz, 1H, aromatic proton), 7.56 (d, J = 6.0 Hz, 1H, aromatic proton), 7.38 (t, J = 6.0, 2H, aromatic proton), 7.20 (m, 1H, aromatic proton), 4.91 (bs, 1H, $CH(^iPr)$), 3.76 (bs, 1H, $CH(^iPr)$), 2.93 (s, 3H, CH_3(DMSO), 2.56 (s, 3H, CH_3(DMSO)), 1.78 (bs, 15H, Cp*), 1.65-1.30 (m, 12H, 4 x $CH_3(^iPr)$). ^{13}C-NMR (100.6 MHz, CD_2Cl_2) δ (ppm): 8.95, 43.13, 44.20, 52.92, 53.19, 53.46, 53.73, 54.00, 95.37, 124.67, 129.36, 133.71, 137.49. Elemental Analysis: Theory: (C, 40.49; H, 5.78; N, 1.57). Found: (C, 40.98; H, 5.15; N, 1.87).

Computational Analysis.

This study was carried out using density functional theory (DFT) with the Gaussian09,[17] implementation of the B3PW91 functional.[18] All geometry optimizations were carried out using tight convergence criteria ("opt=tight") on an ultrafine grid ("int=ultrafine"). The Stuttgart-Dresden (SDD)[19] relativistic effective core potential (RECP) basis set was used for iridium with an additional f polarization function.[20] The def2-TZVP effective core potential (ECP)[21] and basis set was used for the halogens. The 6-31G** basis set[22] was used for all other atoms. Solvation energies were computed with geometries optimized in the gas phase using the SMD method,[23] with dichloroethane as the solvent, as implemented in Gaussian 09. In this method an IEFPCM calculation is performed with radii and electrostatic terms from Truhlar and co-workers' SMD solvation model.[24] Energetics were calculated using the 6-311++G** basis set for all atoms and the SDD basis set with an added f polarization function on iridium. The def2-TZVP ECP and basis set was used for the halogens. All energies are reported in kcal/mol.

Conflicts of interest

The manuscript was written through contributions of all authors. All authors have given approval to the final version of the manuscript. The authors declare no competing financial interests.

Acknowledgements

We acknowledge North Carolina State University and the National Science Foundation (CHE-1664973) for funding and the NCSU Office of Information Technology High Performance Computing Services for computational support.

Notes and references

1. (a) Rakshit, S.; Patureau, F. W.; Glorius, F., *J. Am. Chem. Soc.* **2010,** *132*, 9585-9587; (b) Zhang, J.; Qian, H.; Liu, Z.; Xiong, C.; Zhang, Y., *Eur. J. Org. Chem.* **2014,** *2014*, 8110-8118; (c) Hyster, T. K.; Rovis, T., *J. Am. Chem. Soc.* **2010,** *132*, 10565-10569; (d) Keisuke, M.; Koji, H.; Tetsuya, S.; Masahiro, M., *Chem. Lett.* **2011,** *40*, 600-602; (e) Satoshi, M.; Nobuyoshi, U.; Koji, H.; Tetsuya, S.; Masahiro, M., *Chem. Lett.* **2010,** *39*, 744-746; (f) Guimond, N.; Gouliaras, C.; Fagnou, K., *J. Am. Chem. Soc.* **2010,** *132*, 6908-6909; (g) Luo, C.-Z.; Jayakumar, J.; Gandeepan, P.; Wu, Y.-C.; Cheng, C.-H., *Org. Lett.* **2015,** *17*, 924-927; (h) Morimoto, K.; Hirano, K.; Satoh, T.; Miura, M., *Org. Lett.* **2010,** *12*, 2068-2071; (i) Morimoto, K.; Hirano, K.; Satoh, T.; Miura, M., *J. Org. Chem.* **2011,** *76*, 9548-9551; (j) Jia, J.; Shi, J.; Zhou, J.; Liu, X.; Song, Y.; Xu, H. E.; Yi, W., *Chem. Commun.* **2015,** *51*, 2925-2928; (k) Mochida, S.; Hirano, K.; Satoh, T.; Miura, M., *J. Org. Chem.* **2009,** *74*, 6295-6298; (l) Unoh, Y.; Hashimoto, Y.; Takeda, D.; Hirano, K.; Satoh, T.; Miura, M., *Org. Lett.* **2013,** *15*, 3258-3261; (m) Qi, Z.; Wang, M.; Li, X., *Org. Lett.* **2013,** *15*, 5440-5443; (n) Umeda, N.; Hirano, K.; Satoh, T.; Shibata, N.; Sato, H.; Miura, M., *J. Org. Chem.***2011,** *76*, 13-24; (o) Frasco, D. A.; Lilly, C. P.; Boyle, P. D.; Ison, E. A., *ACS Catal.* **2013,** *3*, 2421-2429.

2. (a) Satoh, T.; Miura, M., *Chem. – Eur. J.* **2010,** *16*, 11212-11222; (b) Song, G.; Wang, F.; Li, X., *Chem. Soc. Rev.* **2012,** *41*, 3651-3678; (c) Kuhl, N.; Schröder, N.; Glorius, F., *Adv. Synth. Catal.* **2014,** *356*, 1443-1460; (d) Shin, K.; Kim, H.; Chang, S., *Acc Chem. Res.* **2015,** *48*, 1040-1052; (e) Yu, D.-G.; Suri, M.; Glorius, F., *J. Am. Chem. Soc.* **2013,** *135*, 8802-8805; (f) Zhang, C.; Zhou, Y.; Deng, Z.; Chen, X.; Peng, Y., *Eur. J. Org. Chem.* **2015,** *2015*, 1735-1744; (g) Park, S. H.; Kwak, J.; Shin, K.; Ryu, J.; Park, Y.; Chang, S., *J. Am. Chem. Soc.* **2014,** *136*, 2492-2502; (h) Wang, N.; Li, R.; Li, L.; Xu, S.; Song, H.; Wang, B., *J. Org. Chem.* **2014,** *79*, 5379-5385; (i) Yang, Y.; Hou, W.; Qin, L.; Du, J.; Feng, H.; Zhou, B.; Li, Y., *Chem. – Eur. J.* **2014,** *20*, 416-420; (j) Gwon, D.; Lee, D.; Kim, J.; Park, S.; Chang, S., *Chem. – Eur. J.* **2014,** *20*, 12421-12425; (k) Gwon, D.; Park, S.; Chang, S., *Tetrahedron* **2015,** *71*, 4504-4511; (l) Mochida, S.; Hirano, K.; Satoh, T.; Miura, M., *Org. Lett.* **2010,** *12*, 5776-5779; (m) Mochida, S.; Hirano, K.; Satoh, T.; Miura, M., *J. Org. Chem.* **2011,** *76*, 3024-3033; (n) Patel, P.; Chang, S., *Org. Lett.* **2014,** *16*, 3328-3331; (o) Kim, H.; Shin, K.; Chang, S., *J. Am. Chem. Soc.* **2014,** *136*, 5904-5907; (p) Suzuki, C.; Hirano, K.; Satoh, T.; Miura, M., *Org. Lett.* **2015,** *17*, 1597-1600; (q) Hull, J. F.; Balcells, D.; Blakemore, J. D.; Incarvito, C. D.; Eisenstein, O.; Brudvig, G. W.; Crabtree, R. H., *J. Am. Chem. Soc.* **2009,** *131*, 8730-8731; (r) Hintermair, U.; Sheehan, S. W.; Parent, A. R.; Ess, D. H.; Richens, D. T.; Vaccaro, P. H.; Brudvig, G. W.; Crabtree, R. H., *J. Am. Chem. Soc.* **2013,** *135*, 10837-10851; (s) Zhou, M.; Schley, N. D.; Crabtree, R. H., *J. Am. Chem. Soc.* **2010,** *132*, 12550-12551; (t) Zhou, M.; Balcells, D.; Parent, A. R.; Crabtree, R. H.; Eisenstein, O., *ACS Catal.* **2012,** *2*, 208-218; (u) Zhou, M.; Hintermair, U.; Hashiguchi, B. G.; Parent, A. R.; Hashmi, S. M.; Elimelech, M.; Periana, R. A.; Brudvig, G. W.; Crabtree, R. H., *Organometallics* **2013,** *32*, 957-965; (v) Hohloch, S.; Kaiser, S.; Duecker, F. L.; Bolje, A.; Maity, R.; Košmrlj, J.; Sarkar, B., *Dalton Trans.* **2015,** *44*, 686-693.

3. (a) Schröder, N.; Wencel-Delord, J.; Glorius, F., *J. Am. Chem. Soc.* **2012,** *134*, 8298-8301; (b) Kuhl, N.; Schröder, N.; Glorius, F., *Org. Lett.* **2013,** *15*, 3860-3863; (c) Schröder, N.; Lied, F.; Glorius, F., *J. Am. Chem. Soc.* **2015,** *137*, 1448-1451; (d) Hwang, H.; Kim, J.; Jeong, J.; Chang, S., *J. Am. Chem. Soc.* **2014,** *136*, 10770-10776; (e) Zhang, P.; Hong, L.; Li, G.; Wang, R., *Adv. Synth. Catal.* **2015,** *357*, 345-349; (f) Qian, G.; Hong, X.; Liu, B.; Mao, H.; Xu, B., *Org. Lett.* **2014,** *16*, 5294-5297; (g) Mei, T.-S.; Wang, D.-H.; Yu, J.-Q., *Org. Lett.* **2010,** *12*, 3140-3143; (h) Li, J.-J.; Mei, T.-S.; Yu, J.-Q., *Angew. Chem.* **2008,** *120*, 6552-6555; (i) Bedford, R. B.; Engelhart, J. U.; Haddow, M. F.; Mitchell, C. J.; Webster, R. L., *Dalton Trans.* **2010,** *39*, 10464-10472; (j) Erbing, E.; Sanz-Marco, A.; Vázquez-Romero, A.; Malmberg, J.; Johansson, M. J.; Gómez-Bengoa, E.; Martín-Matute, B., *ACS Catal.* **2018,** *8*, 920-925.

4. Rakita, P. E., CHEMICAL INDUSTRIES-NEW YORK-MARCEL DEKKER- **1996**, 79-88.

5. Negishi, E.-i.; de Meijere, A., *Handbook of organopalladium chemistry for organic synthesis*. Wiley-Interscience: 2002; Vol. 2.

6. Gribble, G. W., *Acc. Chem. Res.* **1998,** *31*, 141-152.

7. Jeschke, P., *Pest Manage. Sci.* **2010,** *66*, 10-27.

8. Zhang, T.; Qi, X.; Liu, S.; Bai, R.; Liu, C.; Lan, Y., *Chem. – Eur. J.* **2017,** *23*, 2690-2699.

9. Lehman, M. C.; Gary, J. B.; Boyle, P. D.; Sanford, M. S.; Ison, E. A., *ACS Catal.* **2013,** *3*, 2304-2310.

10. Engelman, K. L.; Feng, Y.; Ison, E. A., *Organometallics* **2011,** *30*, 4572-4577.

11. For comparable KIE values: (a) Ref. 3a; (b) Wang, L.; Ackerman L., *Chem. Commun.*, **2014,** *50*, 1083-1085; (c)

12. (a) Castanet, A.-S.; Colobert, F.; Broutin, P.-E., *Tetrahedron Lett.* **2002,** *43*, 5047-5048; (b) Küpper, F. C.; Feiters, M. C.; Olofsson, B.; Kaiho, T.; Yanagida, S.; Zimmermann, M. B.; Carpenter, L. J.; Luther, G. W.; Lu, Z.; Jonsson, M.; Kloo, L., *Angew. Chem. Int. Ed. Engl.* **2011,** *50*, 11598-11620; (c) Küpper, F. C.; Feiters, M. C.; Olofsson, B.; Kaiho, T.; Yanagida, S.; Zimmermann, M. B.; Carpenter, L. J.; Luther, G. W.; Lu, Z.; Jonsson, M.; Kloo, L., *Angew. Chem.* **2011,** *123*, 11802-11825; (d) Muñiz, K.; García, B.; Martínez, C.; Piccinelli, A., *Chem. – Eur. J.* **2017,** *23*, 1539-1545.

13. (a) Barluenga, J.; González, J. M.; Campos, P. J.; Asensio, G., *Angew. Chem. Int. Ed. Engl.* **1985,** *24*, 319-320; (b) Barluenga, J., *Pure Appl. Chem.* **1999,** *71*, 431-436; (c) Ashikari, Y.; Shimizu, A.; Nokami, T.; Yoshida, J.-i., *J. Am. Chem. Soc.* **2013,** *135*, 16070-16073.

14. (a) Gorelsky, S. I.; Lapointe, D.; Fagnou, K., *J. Am. Chem. Soc.* **2008,** *130*, 10848-10849; (b) Walsh, A. P.; Jones, W. D., *Organometallics* **2015,** *34*, 3400-3407; (c) Gorelsky, S. I.; Lapointe, D.; Fagnou, K., *J. Org. Chem.* **2012,** *77*, 658-668; (d) Jiang, J.; Ramozzi, R.; Morokuma, K., *Chem. – Eur. J.* **2015,** *21*, 11158-11164; (e) Ackermann, L., *Chem. Rev.* **2011,** *111*, 1315-1345.

15. White, C., Yates, A. , Maitlis, P. M. and Heinekey, D. M. , (η5-Pentamethylcyclopentadienyl)Rhodium and -Iridium Compounds. In *Inorganic Syntheses*, 2007.

16. Wik, B. J.; Rømming, C.; Tilset, M., *J. Mol. Catl. A: Chem.* **2002,** *189*, 23-32.

17. Frisch, M.; Trucks, G.; Schlegel, H.; Scuseria, G.; Robb, M.; Cheeseman, J.; Scalmani, G.; Barone, V.; Mennucci, B.; Petersson, G. *Gaussian 09 package*, 2009.

18. Parr, R. G.; Yang, W., Density-Functional Theory of Atoms and Molecules, vol. 16 of International series of monographs on chemistry. Oxford University Press, New York: 1989.

19. Andrae, D.; Haeussermann, U.; Dolg, M.; Stoll, H.; Preuss, H., *Theor. Chim. Acta.* **1990,** *77*, 123-141.

20. (a) Hehre, W. J.; Ditchfield, R.; Pople, J. A., *J. Chem. Phys.* **1972,** *56*, 2257-2261; (b) Dolg, M.; Stoll, H.; Preuss, H.; Pitzer, R. M., *J. Chem. Phys.* **1993,** *97*, 5852-5859.

21. (a) Hay, P. J.; Wadt, W. R., *J. Chem. Phys.* **1985,** *82*, 299-310; (b) Hay, P. J.; Wadt, W. R., *J. Chem. Phys.* **1985,** *82*, 270-283; (c) Wadt, W. R.; Hay, P. J., *J. Chem. Phys.* **1985,** *82*, 284-298.

22. (a) Rassolov, V. A.; Ratner, M. A.; Pople, J. A.; Redfern, P. C.; Curtiss, L. A., *J. Comput. Chem.* **2001,** *22*, 976-984; (b) Rassolov, V. A.; Pople, J. A.; Ratner, M. A.; Windus, T. L., *J. Chem. Phys.* **1998,** *109*, 1223-1229; (c) Krishnan, R.; Binkley, J. S.; Seeger, R.; Pople, J. A., *J. Chem. Phys.* **1980,** *72*, 650-654.

23. Marenich, A. V.; Cramer, C. J.; Truhlar, D. G., *J. Phys. Chem. B* **2009,** *113*, 6378-6396.

24. Tomasi, J.; Mennucci, B.; Cammi, R., *Chem. Rev.* **2005,** *105*, 2999-3094.

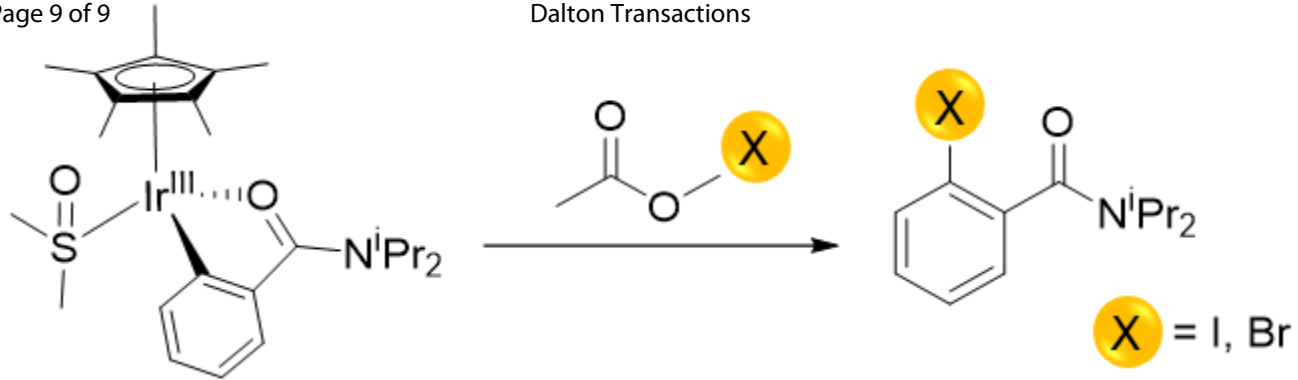
O
S
Ir^III
O
N^iPr2
O
O
X
X
O
N^iPr2
X = I, Br